


# Establishment of a design study for comprehensive hydrodynamic optimisation in the preliminary stage of the ship design

Myo Zin Aung, Amin Nazemian , Evangelos Boulougouris, Haibin Wang, Suleyman Duman and Xue Xu

Department of Naval Architecture, Ocean and Marine Engineering, Maritime Safety Research Centre (MSRC), University of Strathclyde, Glasgow, UK

## ABSTRACT

An automated practical multi-objective optimisation scheme is proposed for ship hull modification. A shift transformation and a self-blending method are sequentially performed based on resistance objectives at multi-design speeds. The Lackenby variation alters hull forms and produces initial designs. Subsequently, self-blending method combines obtained ships to cover design space. All processes are automated by MATLAB coding that connects the ©Maxsurf modeller and ©Maxsurf Resistance in the case of panel method resistance calculation. After whole shape optimisation, the platform defines ship portions in the stern and bow regions. Particularly, an approximation modelling Least-Square approach is investigated to construct a surrogate model. Optimisation results indicate 11.26% cost function reduction contributes to 16.23% resistance reduction at lower speed and 6.12% resistance reduction at higher speed for a passenger catamaran boat. Thus, the developed in-house optimisation code provides an optimal and cost-effective solution for hydrodynamic optimisation in the preliminary stage of ship design.

## ARTICLE HISTORY

Received 29 November 2022  
Accepted 25 April 2023

## KEYWORDS

Total resistance; Ship hull optimisation; Lackenby variation method; Self-blending method; Panel method

## Nomenclature

$B$	Demihull beam
$C_m$	Midship coefficient
$C_b$	Block coefficient
$C_T$	Total resistance coefficient
$C_v$	Viscous resistance coefficient
$C_w$	Wave-making resistance coefficient
$C_f$	Friction resistance coefficient
$k$	Form factor
LCB	Longitudinal Centre of Buoyancy
KB	Keel to buoyancy distance
Lwl	Waterline length
Lpp	Length Between Perpendicular
Loa	Length overall
$R_t$	Total resistance
$R_w$	Wave-making resistance
$R_n$	Reynolds number
$T$	Draft
$U$	Ship speed
$W_t$	Cost function weight
$\alpha$	Blending ratio
$\Delta$	Displacement
$\Delta_{\text{new}}$	Displacement new design
$\Delta_{\text{org}}$	Displacement original design
$\nu$	Kinematic viscosity
$\rho$	Water density

## 1. Introduction



Multi-Disciplinary Design Optimisation (MDO) has been recently accomplished in different industrial projects to improve the performance of the products. Using the MDO method in engineering design and optimisation takes high computational costs and time. The marine industry has been forced to minimise its environmental footprint. Global recession and stricter regulations increase the competition between companies, yield rapid innovation and improve design performance. Accordingly, the marine industry

needs an optimisation platform in the field of shape optimisation to improve ship efficiency without the mentioned computational limitations. Nazemian and Ghadimi (2019a, 2019b, 2020a, 2020b, 2021a) employed simulation-based optimisation platforms for ship resistance and seakeeping performance improvement. Lamently, the applied calculations were extremely expensive and time-consuming. Besides, software and code restrictions restricted the research in the field of hydrodynamic optimisation problems.

The present paper proposes an automated optimisation framework for ship hull form modification at two different multi-design speeds. Thus far, the technique of metamodel (i.e. surrogate model) is adopted to solve this problem (Peri and Campana 2005; Feng et al. 2018), which is used to create a fast analysis module by approximating the existing computer simulation model to achieve more efficient analysis. This paper aims to improve a new simple and effective software to optimise different hull forms without user intervention, which yields to fully automatic process.

## 2. Background

In the preliminary stage of ship design, a fast and accurate optimisation platform is more important than local hull form deformation. Global optimisation methods are performed to calculate the general specifications of ships such as Length, Breadth, Draft, Depth, block coefficient ( $C_b$ ), etc. There is an extensive investigation of ship design and hull form optimisation (Zakerdoost et al. 2013; Zhang and Zhang 2018). However, an optimal and cost-effective approach to hydrodynamic optimisation is required. Also, a combination of two hull form transformation methods is proposed and investigated to represent a successful optimisation. The Lackenby variation method alters hull forms and produces initial designs distributed in the design space. After that, the blending method combines the

**CONTACT** Amin Nazemian  amin.nazemian@strath.ac.uk  Department of Naval Architecture, Ocean and Marine Engineering, Maritime Safety Research Centre (MSRC), University of Strathclyde, Montrose St., Glasgow G4 0LZ, UK

© 2023 The Author(s). Published by Informa UK Limited, trading as Taylor & Francis Group

This is an Open Access article distributed under the terms of the Creative Commons Attribution License (<http://creativecommons.org/licenses/by/4.0/>), which permits unrestricted use, distribution, and reproduction in any medium, provided the original work is properly cited. The terms on which this article has been published allow the posting of the Accepted Manuscript in a repository by the author(s) or with their consent.

obtained ships to cover all design space (Feng et al. 2009; Hong et al. 2017). Accordingly, a MATLAB code is developed to produce different hull forms and make connections between software. In some cases, it is needed to alter a portion of ship geometry in stern or bow regions. Therefore, a novel method is applied to make flexible alterations in every region that the user wants to modify.

Nazemian and Ghadimi (2020b) proposed a surrogate model approach for the side hull arrangement optimisation of a trimaran hull. The mentioned paper optimised the resistance and seakeeping of trimaran ships at two cruise and sprint speeds. Another newly published paper by Nazemian and Ghadimi (2021b) conducted trimaran hull form optimisation by D-optimal design study and Slender Body Method (SBM) for resistance calculation. They performed resistance calculations without considering other parts of the design spiral components. Yildiz et al. (2020) investigated the positioning of trimaran outriggers using experimental and numerical analysis. Their work resulted from a case study outrigger optimisation and good compliance of numerical and test data. Zhang et al. (2018) by using the Latin hypercube sampling method and approximation approach, optimised a Wigley-shaped hull form and DTMB5512 model. Zong et al. (2018) developed a CFD-Based optimisation process for trimaran hulls by combining different disciplines. Ship geometry parameterisation is performed through the self-blending method and is connected with the CFD solver and MIGA optimiser algorithm. Li et al. (2016, 2012) established a multi-disciplinary ship design optimisation by defining a metamodel approach. They used Single-Parameter Lagrangian Support Vector Regression (SPL-SVR) to explore design space and improved the seakeeping performance of the ships during the conceptual design stage. Villa et al. (2021) established an optimisation process using the surrogate model optimisation approach and FFD parameterisation method for calm water resistance optimisation. The obtained results acquired a 10% resistance reduction of the benchmark DTC hull.

The Energy Efficiency Design Index (EEDI) proposed via International Maritime Organisation (IMO) causes obligations of low-emission ship design (Papanikolaou 2010; Boulougouris et al. 2021). The ship design process extends at different targets in the case of optimisation iterations (Wang et al. 2021). Priftis et al. (2016, 2020) conducted a multi-objective optimisation problem for a container ship according to internal and external ship capacity and energy efficiency improvement. Papanikolaou et al. (2010a) established a multi-objective design optimisation of an AFRAMAX tanker. Their objectives included cargo volume, the mean oil-outflow parameter and the steel weight of the cargo block. A successful design study procedure was developed by Papanikolaou et al. through the automation of NAPA and POSEIDON software with ModeFRONTIER. An optimisation process considering uncertainty analysis was conducted by Priftis et al. (2020). The method was applied on a Ro-Pax vessel as a case study with regard to the total resistance, required freight rate and steel weight reduction. Grigoropoulos et al. (2021) proposed a mixed-fidelity design optimisation using a potential flow solver and CFD analysis. The parametric design has been implemented via CAESES software and an optimisation process was conducted through a Genetic Algorithm and potential flow code. An Artificial Neural Network (ANN) regression tool was carried out to build a surrogate model on the extracted design of the Reynolds-Averaged Navier-Stokes Equations (RANS) solver. A combination of the mentioned process yields a reasonably time-consuming optimisation process. Deng et al. (2021) hold a comprehensive optimisation on a bulk carrier ship using empirical methods for resistance, seakeeping, and manoeuvring targets. Nevertheless, their joint optimisation method did not browse other areas of the design space and the possibility of different hull forms. Mittendorf and Papanikolaou (2021)

optimised fast catamarans based on non-linear Rankine panel method resistance calculation and empirical correction for stern flow. The surrogate model study and genetic algorithm optimisation were conducted on parametrised catamaran models.

Duman et al. (2023) using a RANSE-based double-body approach simulated a passenger-fast ferry catamaran in shallow water. However, the cost- and time-consuming disadvantages of this numerical analysis won't be a suitable approach for an optimisation study. An accurate and effective prediction technique for assessing the resistance performance plays an important role in the hydrodynamic-based Multidisciplinary Design Optimisation (MDO) for ships (Kim et al. 2007). Therefore, a balance between accuracy and time should be implemented. Although some designers have combined the optimisation techniques for pursuing the CFD-Based optimisation of ship hulls (Peri et al. 2001; Nazemian and Ghadimi 2021c; Shi et al. 2021), this approach is very time-consuming and much computational effort is demanded.

According to the surveyed literature review, it is inevitable that a fast and more practical optimisation platform can be developed in the field of the marine industry. A significant advantage of the present method is the combination of shift transformation and a novel self-blending method, which generates different hull forms. The generated ship geometries fulfill all shape possibilities in design space considering fairness and smoothness of hull forms. The mentioned software is fully automated without the need to spend tedious time and effort on hull form parameterisation. In other words, one may define an IGES or \*.msd format file of initial ship geometry and finally take optimum design after a reasonably short amount of time.

Accordingly, the total resistance of the present effort is computed by the panel method. The validity of the applied resistance calculation will be approved by available experimental data. To accomplish this task, a Slender Body Method is applied. Total resistance at 12 knots and total resistance at 22 knots are targets of multi-objective optimisation. Waterline length (LWL), demi-hull beam (B), Draft (T), Longitudinal centre of buoyancy (LCB), Midship coefficient (Cm) and Demi-hull transversal distance (DemiOffset) are design variables of shift transformation. Twenty best designs of transformation method define as parents of the self-blending method. Every parent generates 21 children according to 7 children for the whole shape, 7 children for the or aft region and 7 children for fore region modification. Self-blending method displaces parents' control points in X, Y and Z directions. Finally, the results of hull form optimisation are presented and discussed. The initial and optimised hulls are compared, and the optimisation framework and its effectiveness are verified.

### 3. Problem definition

Developing a more practical and efficient optimisation platform is the basic mission of the present paper. One of the important goals is the introduction of a fast-engineering tool to extract an optimal hull form in the preliminary stage of the ship design. A global optimisation approach is established to reduce the total resistance of a catamaran boat vessel (ongoing EU-funded project TrAM (<https://tramproject.eu/>)) at two design speeds. A panel method for the resistance calculation is applied to compute the outputs of the design study. In addition, a Least Square regression model is implemented to extract other interesting designs. Statistical models are valuable tools to support a wide scope of activities in modern engineering design, especially ship design optimisation (Jeong and Kim 2013; Zhang et al. 2013). Multi-dimensional movement of control points in B-spline hulls and section representation alters the hull and generates new geometry. The principal dimensions of the passenger catamaran boat are shown in Table 1

**Table 1.** Principal dimensions of the catamaran boat (Papanikolaou et al. 2020; Xing-Kaeding and Papanikolaou 2021).

Dimension	Nondim.	Nondim. Value
Separation (s)	s/Lpp	0.227
Draught (T)	T/Lpp	0.040
KB	KB/Lpp	0.026
LCB	LCB/Lpp	0.460

**Table 2.** Design variables of the study.

Specifications	Symbol	Optimisation parameter
Overall length (m)	Loa	–
Waterline length (m)	$L_{wl}$	Design variable
Demi hull Beam (m)	$B$	Design variable
Draft (m)	$T$	Design variable
Demi-hull transverse distance (m)	$DT$	Design variable
Block coefficient	$C_b$	–
Max section area coefficient	$C_m$	Design variable
Longitudinal Centre of Buoyancy	LCB (% of $L_{wl}$ )	Design variable
Displacement (Ton)	$\Delta$	Constraint
Total beam (m)	$(DT \times 2) + B$	Constraint

(Papanikolaou et al. 2020; Xing-Kaeding and Papanikolaou 2021) and design variables of the study are depicted in Table 2. Also, Figure 1 displays a 3D view of the mentioned hull with network control points.

Six design variables of this design study include Waterline length (Lwl), Total Beam Demi-hull ( $B$ ), Draft ( $T$ ), Midship coefficient ( $C_m$ ), Longitudinal centre of buoyancy (LCB) and Demi-Hull Distance (DemiOffset). Index 0 represents the initial value of a parameter for baseline hull forms. These parameters and their levels are presented below as input for the optimisation study:

#### Inputs:

LWL = [29, LWL0, 31]	3-Level	LCB = [0.51, LCB_ND0, 0.525]	3-Level
$B$ = [2.05, 2.1, B0, 2.23]	4-Level	$C_m$ = [0.77, $C_{m0}$ , 0.78, 0.79]	4-Level
$T$ = [1.15, 1.2, 1.25]	3-Level	DemiOffset = [3.35, DemiOffset0, 3.45]	3-Level

The output of the optimisation process is resistance at 12 knots and resistance at 22 knots, which are represented by a weighting cost function:

$$\text{Cost function} = \left( \left( \frac{R_{t_e}}{R_{t_{LowFn0}}} \right) W_{t_{LowFn}} + \left( \frac{R_{t_{HighFn}}}{R_{t_{HighFn0}}} \right) W_{t_{HighFn}} \right) \times \left( \frac{\text{Disp0}}{\text{Disp\_get}} \times \frac{1}{1000} \right) \quad (1)$$

$R_{t_{LowFn}}$  is the resistance at a low Froude number, which indicates resistance at 12 knots.  $R_{t_{HighFn}}$  represents the resistance at a high Froude number that contributes to resistance at 22 knots. Disp0 and Disp\_get are respectively displacements of the initial hull and displacement of the new hull, which are calculated from hydrostatic data. Shape modification and change in ship hull geometry are accomplished by constraining the difference at the displacement of less than 1%. If displacement is the only constraint, the length, beam and draft are automatically actualised to accommodate the redistributed volume. As a result, the displacement constraint is defined as follows:

$$\left| \frac{\Delta_{\text{new}} - \Delta_{\text{org}}}{\Delta_{\text{org}}} \right| \leq 0.01 \quad (2)$$

where  $\Delta_{\text{new}}$  is the displacement of the new design and  $\Delta_{\text{org}}$  is the displacement of the original design. Another constraint of the present study is the total beam of the catamaran to satisfy port requirements, therefore

$$2 \times \text{Demihull offset} + \text{demihull beam} \leq 9 \quad (3)$$

where Demi-hull offset is the distance between the centreline of each demi-hull.

### 3.1. Resistance calculation method: the Slender Body Method (SBM)

The use of linear, slender body theory is a common approach in the numerical modelling of wave resistance for slender hull types, such

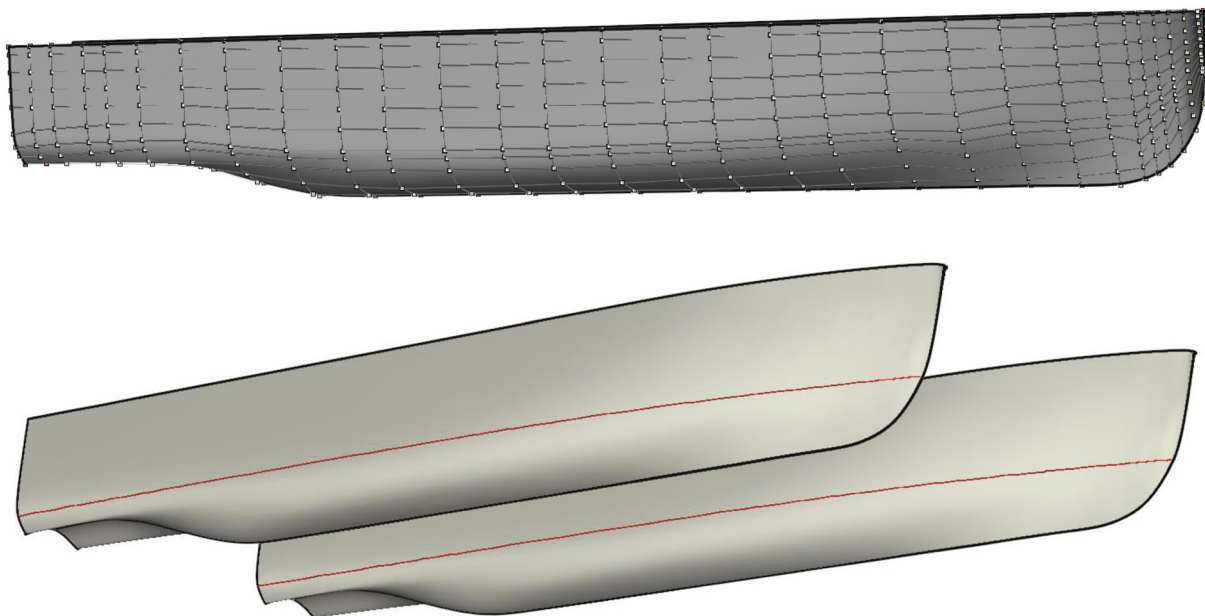


**Figure 1.** Passenger catamaran of the design study (top) 12 rows and 31 columns of control points for Demi-hull geometry (bottom) 3D view of the catamaran. (This figure is available in colour online.)

as ships and submarines. This is because these methods can provide fast and accurate solutions to the wave resistance problem for these types of hulls. The hull shape can be approximated as a three-dimensional panel mesh that is uniform along the length of the hull. Numerical models that use linear, slender body theory typically involve discretising the hull into a series of panels and then solving for the flow around each panel using potential flow theory. The solutions for each panel are then combined to calculate the total wave resistance of the hull.

Mitchell (1898), Wigley (1933) and Eggers (1955) developed this code for various hull forms and this method can now be applied to a wide range of hull forms including multihull ships. Insel (1990) and Insel and Molland (1992), Cong and Hsiung (1990) are among those who applied the more developed method. The work described here uses the method developed by Insel and Molland (1992) in which the wave resistance is calculated from the description of the far-field wave system using Eggers coefficients. Also, the ship resistance calculation is based on the proposed method by Couser et al. (1996, 1998). For the transom-sterned hulls, this method joins a 'virtual appendage' which models the air gap behind the transom and simulates the turbulent viscous wake behind the transom at slow speeds.

This method can be applied to under-studied catamaran ships. The formulation set-up of thin ship theory is hereby explained. The total drag is made up of two components: the viscous drag due to the movement of the ship through a viscous fluid and the wave-making resistance due to the movement of the ship on the free surface. The wave-making drag results from energy dissipation in the water surface waves. The total drag coefficient is given as

$$C_T = C_v + C_w \quad (4)$$

where  $C_v$  is the viscous drag coefficient and  $C_w$  is the wave-making drag coefficient. The viscous drag is composed of frictional drag and form drag, i.e.  $C_v = (1 + k)C_f$ , where  $C_f$  is the frictional drag coefficient and  $k$  is the form factor that calculates by Molland formulae. The frictional drag coefficient is calculated by ITTC57 as follows:

$$C_f = \frac{0.075}{(\log Rn - 2)^2} \quad (5)$$

where  $Rn$  is the Reynolds number given by

$$Rn = \frac{UL}{\nu} \quad (6)$$

where  $U$  is the ship's speed,  $L$  is the ship's length and  $\nu$  is the kinematic viscosity of the water. The length of the centre hull of a trimaran ship is normally different from that of the side hulls. The wave-making drag is based on the wave energy flux far from the ship hull. The equation for the wave-making drag is

$$R_w = \frac{\pi}{2} \rho U^2 \int_{-\pi/2}^{\pi/2} |A(\theta)|^2 \cos^3 \theta d\theta \quad (7)$$

where  $\rho$  is the density of the water,  $\theta$  is the angle between the direction of the moving ship and that of a propagating wave and  $A(\theta)$  is the amplitude function specific to the hull shape. Herein, a comparison will be conducted between the experiment results of the TrAM catamaran and slender body method (Figure 2) for both bare hull and appended hull for validation of the resistance calculation method.

The obtained results generally confirmed the validity of the herein-applied resistance calculation methods and optimisation procedures. The comparison of bare hull results of SB and experiment data at speeds 12 and 22 knots shows a 1.5% and 1.7%

discrepancy, respectively. Accordingly, one may indicate good compliance of comparison and validity of the SB method for the rest of optimisation study.

### 3.2. Design of experiments on the shift transformation method

Design of Experiments (DOE) is a powerful tool that can be utilised in the ship design. This technique extracts interactive effects of many factors that could affect the overall design variables, such as beam, draught and length, and provide a full insight into the interaction between parameters and responses. In the current paper, the multi-level sampling tool is used to distribute produced design from the Lackenby variation method. Shift transformations is a geometry modification tool to deform or shift geometries with regard to the principal axes  $x$ ,  $y$  and  $z$ . The Lackenby variation method or Lackenby shift transformation is the geometry parametrisation method in the current paper (Lackenby 1950). The Lackenby variation method involves generating a set of related hull forms by making small, incremental changes to the design parameters of the original hull form. The changes are typically applied to the longitudinal and transverse sections of the hull and may involve altering the shape of the hull. This process involves moving the columns fore and aft, while not changing the section shapes (unless scaling them), i.e. all the  $y$ -coordinates are moved by the ratio of the beams and all the  $z$ -coordinates by the ratio of the drafts (Roh and Lee 2017; Nazemian and Ghadimi 2021b). The transformation moves stations fore and aft until the required parameter(s) specifications are met. Section transformation defines the formulae  $\Delta y = \Delta x(x)$ . This means, that at a specific  $x$ -position of the hull, there is a shift of the geometry in the  $x$ -direction by using the corresponding  $y$ -value. A positive  $y$ -value means a forward shift and a negative value signals a backward shift. A key quality of this function is that it maintains the fairness of the hull to a very high degree during the transformation process.

### 3.3. Blending method

The blending method alters geometry by moving the control points. Parametric transformation is performed to create a hull, which is blended from two other parent hull forms. This method combines two hulls by using a blending function and creates a new hull. The blended hull control point coordinates are proportional between the two other coordinate sets, in the ratio specified by the blending ratio ( $\alpha$ ), ranging from 0 to 1 (entirely hull 1, to entirely hull 2). 12 rows and 31 columns of control points include surfaces of the hull. The blending function in three directions is expressed as follows:

$$CP_{\text{new}}(x_{\text{new}}, y_{\text{new}}, z_{\text{new}}) = \alpha \times CP_i(x_i, y_i, z_i) + (1 - \alpha)CP_j(x_j, y_j, z_j) \quad (8)$$

Here,  $CP$  indicates the control point,  $\alpha$  is the blending ratio and  $i$  and  $j$  are the number of hulls for blending execution. New positions of control points for new hulls are found by using relation 8.

An example of extracting a blending curve from two simple quadrant curves is depicted in Figure 3. In the current example, the blending ratio is 0.5. It should be noticed that generated curves in 3D shapes are not exactly as shown in Figure 3. The generated surfaces from new control points construct the blended sections which alter in three directions. The mentioned definition is presented in Figure 4. In Figure 4, sections of two parents ( $P1$ ,  $P2$ ) are blended in  $YZ$ ,  $Y$  and  $Z$  directions to generate the child section. Besides, these control points combine in the  $X$  direction, which produces three-dimensional curve blending. Accordingly, various hull

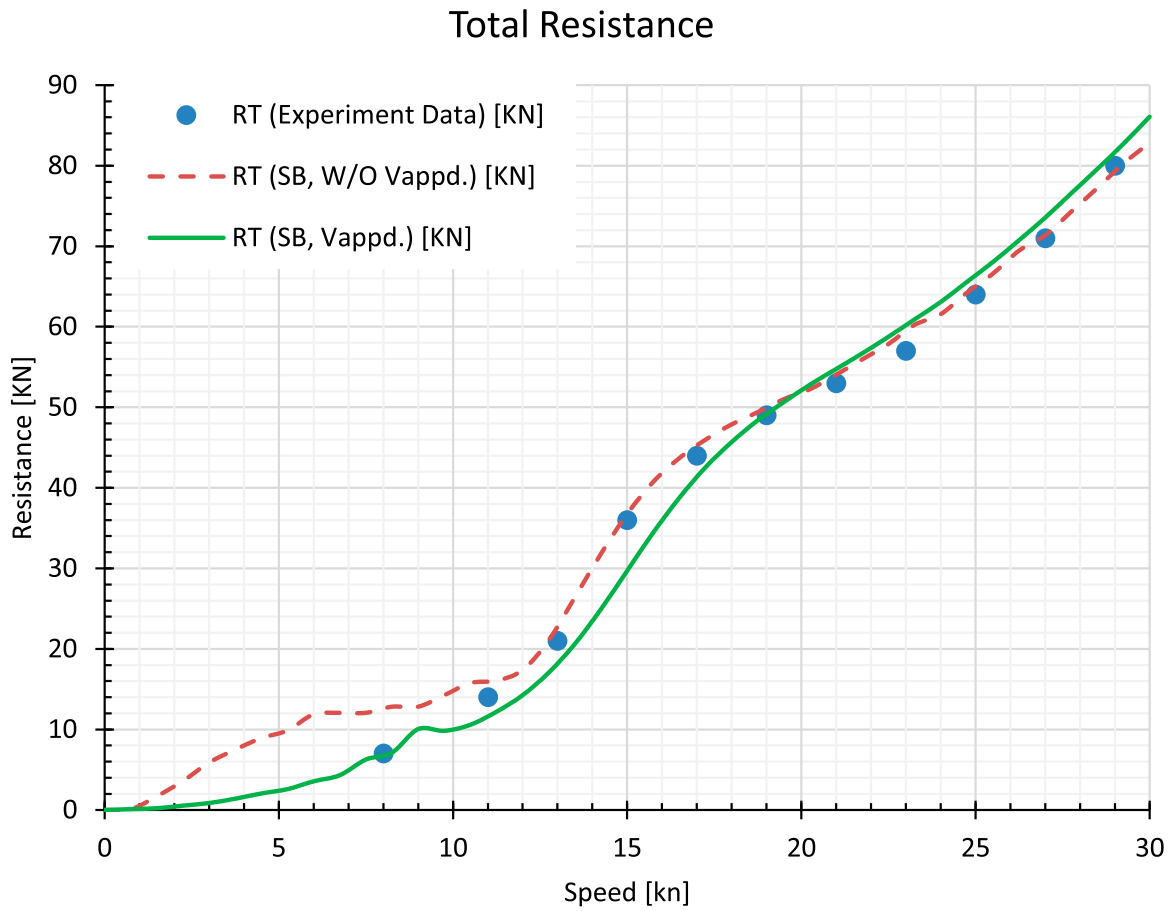


**Figure 2.** Comparison of the computed SB method results against experimental data (Papanikolaou et al. 2020; Xing-Kaeding and Papanikolaou 2021). (This figure is available in colour online.)

forms are reconstructed during the self-blending method application in the design study process.

To extend design space, the self-blending approach is implemented in the aft and fore regions specifically. Figure 5 shows different parts of the demi hull with 9 sections for the aft

and 12 sections for the fore region. In general, users can control several portions and sections voluntarily to generate many geometries. For example, these control points can be combined in every direction solely ( $X$ ,  $Y$  and  $Z$ ) or combined two by two such as  $XY$ ,  $XZ$  and  $YZ$ . Therefore, every parent can generate seven children (relations 5–7). This scenario implements the bow and aft region of geometry to investigate the effect of portion alteration on hull form optimisation. Relations 5, 6 and 7 depict different hull form generation for the whole body, Aft and Fore region for parent  $P1$  and parent  $P2$ .

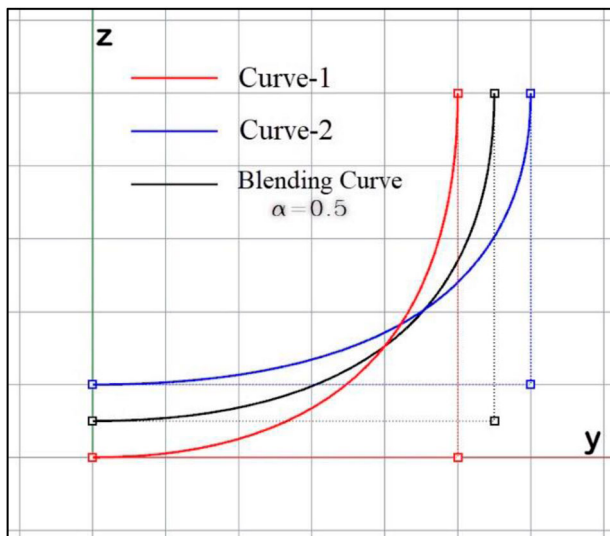
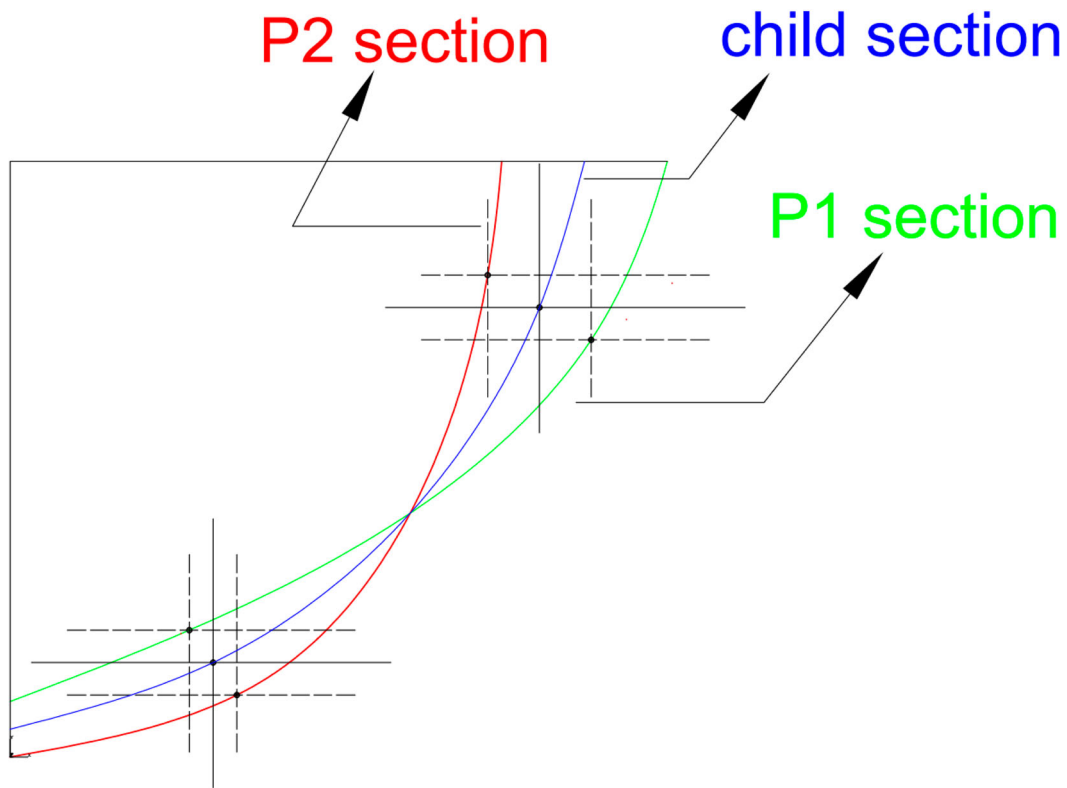


**Figure 3.** Example of using the blending method to extract blending curves from two arcs. (This figure is available in colour online.)

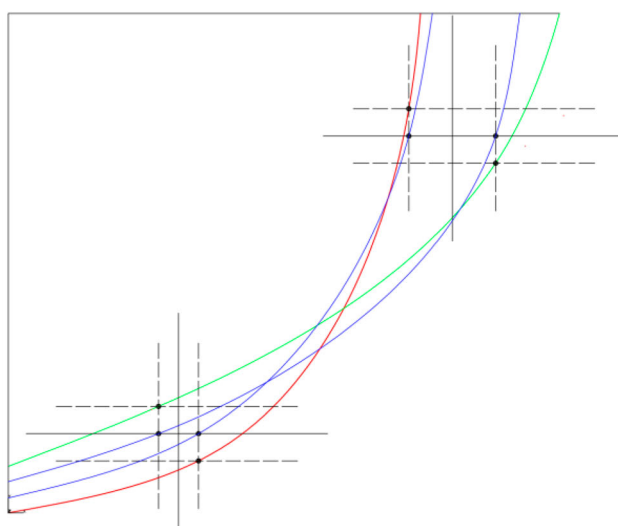
$$\begin{aligned}
 \text{Whole body} = & P1(xyz)P2(xyz) + P1(x)P2(x) + P1(y)P2(y) \\
 & + P1(z)P2(z) + P1(xy)P2(xy) \\
 & + P1(xz)P2(xz) + P1(yz)P2(yz) \quad (9)
 \end{aligned}$$

$$\begin{aligned}
 \text{Aft region} = & P1a(xyz)P2a(xyz) + P1a(x)P2a(x) \\
 & + P1a(y)P2a(y) + P1a(z)P2a(z) \\
 & + P1a(xy)P2a(xy) + P1a(xz)P2a(xz) \\
 & + P1a(yz)P2a(yz) \quad (10)
 \end{aligned}$$

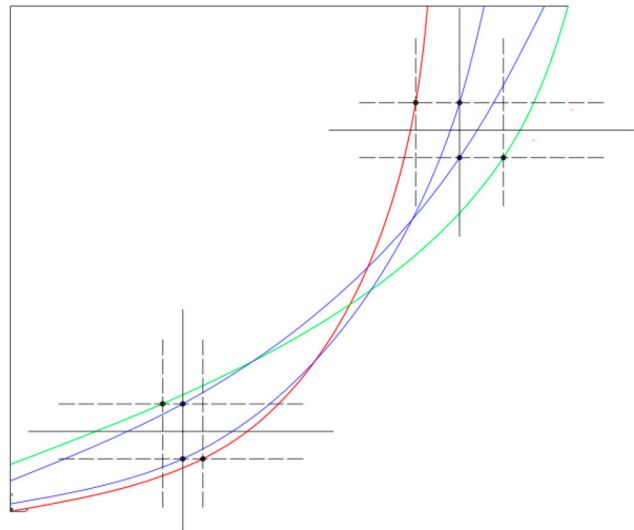
$$\begin{aligned}
 \text{Fore region} = & P1f(xyz)P2f(xyz) + P1f(x)P2f(x) \\
 & + P1f(y)P2f(y) + P1f(z)P2f(z) \\
 & + P1f(xy)P2f(xy) + P1f(xz)P2f(xz) \\
 & + P1f(yz)P2f(yz) \quad (11)
 \end{aligned}$$



(a) Self-blending of two parent's control points (P1, P2) and making one child curve the in y-z direction



(b) y direction self-blending



(c) z direction self-blending

**Figure 4.** Self-blending of one section of two parents (P1, P2) in (a) the YZ direction, (b) the Y direction, (c) the Z direction. (a) Self-blending of two parent's control points (P1, P2) and making one child curve in the y-z direction (b) the y-direction self-blending; (c) the z-direction self-blending. (This figure is available in colour online.)

Control of the shape modification through section curves and their control points is easier than shape parametrisation by the hull surfaces. Therefore, the number of design variables is reduced and the complexity of geometry parameterisation is extricated. Furthermore, this approach reduces designer dependence on the experience or lack of detailed data, especially at the preliminary or concept level of the ship design. Briefly, the advantages of this method are as follows:

- (1) Significant time and effort savings by removing the need for a parametric model.
- (2) The process is highly automated.
- (3) Fairness and smoothness of hull forms remain during the design generation.
- (4) The combination of shift transformation and the self-blending method cover all possibilities of geometry variation even if global or local shape modification.

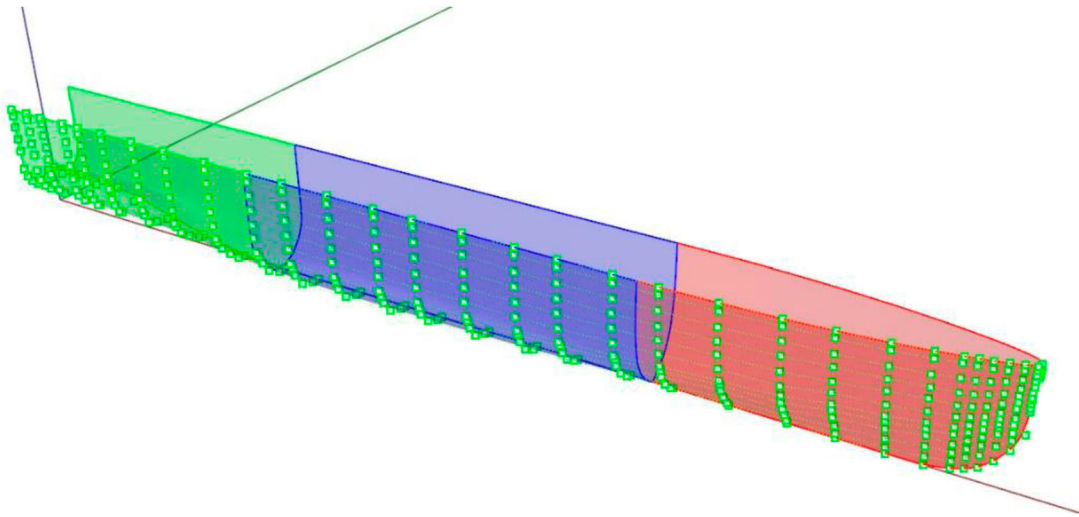


**Figure 5.** Aft, Fore and middle body of the demi-hull of a catamaran. (This figure is available in colour online.)

An example of extracting a blending curve is depicted in Figure 6 for two designs. In the current example, the blending ratio is taken as 0.5. The generated surfaces from the new control points construct the blended sections, which alter in three directions. The 3D geometries of three designs are presented in Figure 7 in blue, red and green colours.

### 3.5. Optimisation process

A series of simulations are carried out to build a surrogate model or (response surface) which presents a relationship between design variables and objectives. The simulation domain is a range defined by the minimum and maximum limits of the design

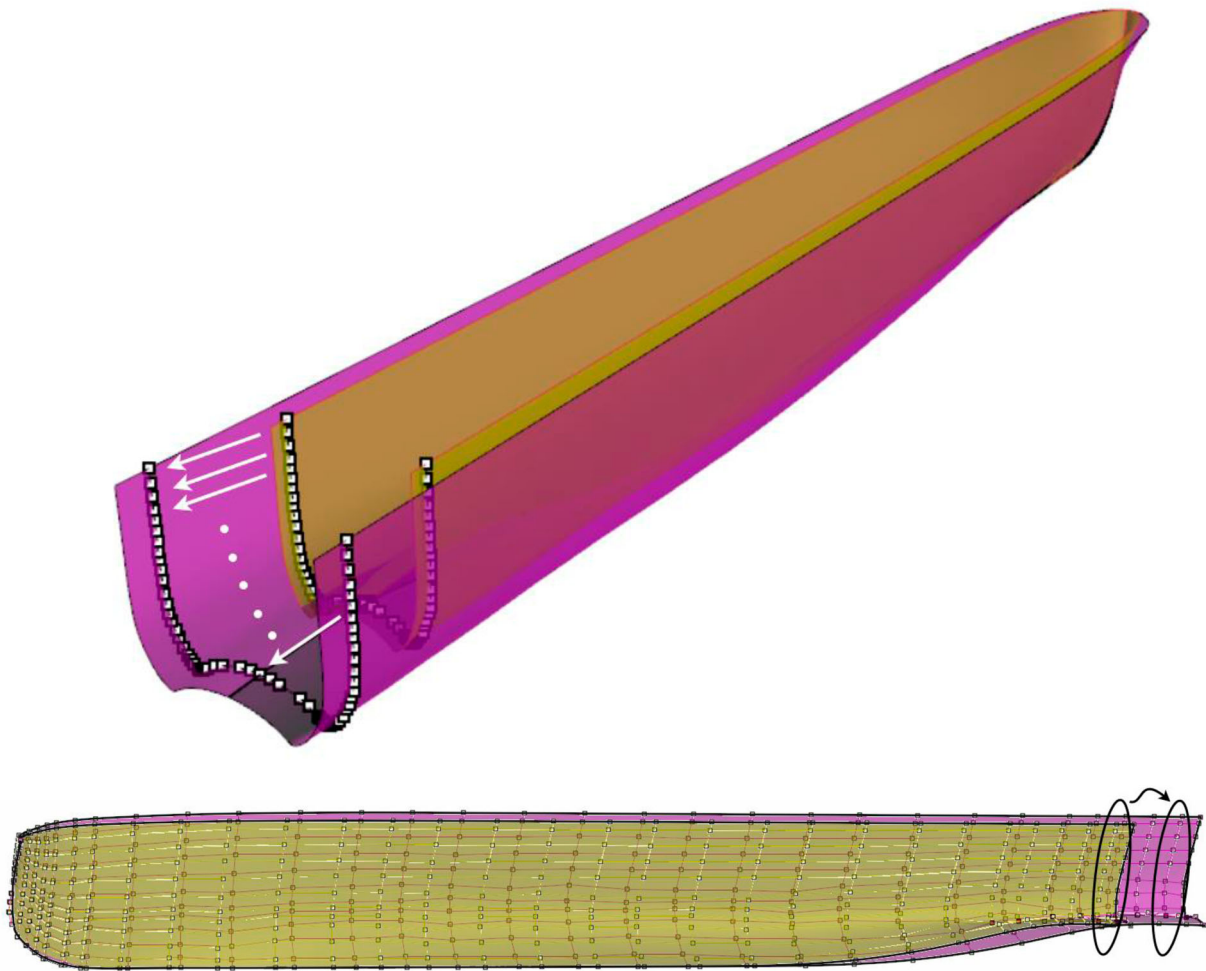


**Figure 6.** Example of hull form alteration and control points movements, consequently new surface generation. (This figure is available in colour online.)

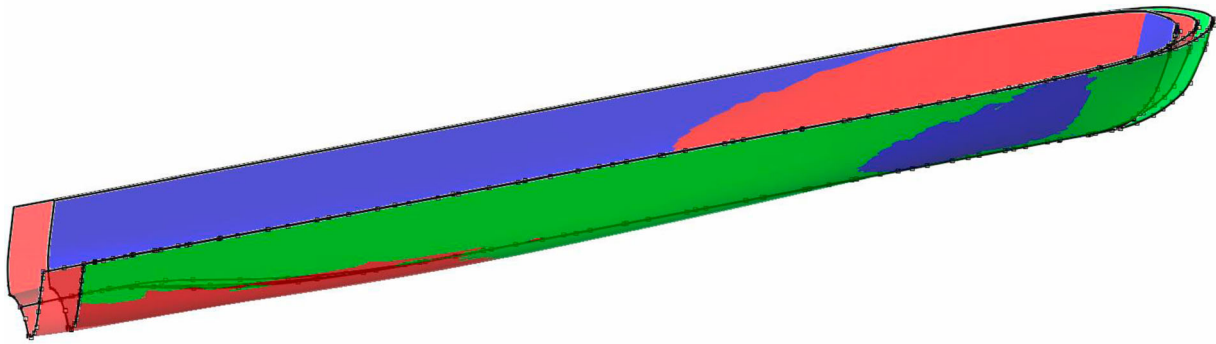


**Figure 7.** The 3D shape of three design generations via a self-blending method. (This figure is available in colour online.)

variables. Levels of a variable are different values of a variable at which the simulations must be carried out. Simulation design is a set of simulations defined by a matrix consisting of different levels

of variables. Responses are the total resistance at two independent speeds. The surrogated-based approach is employed to extract design space and find the optimum design. The Cubic Least

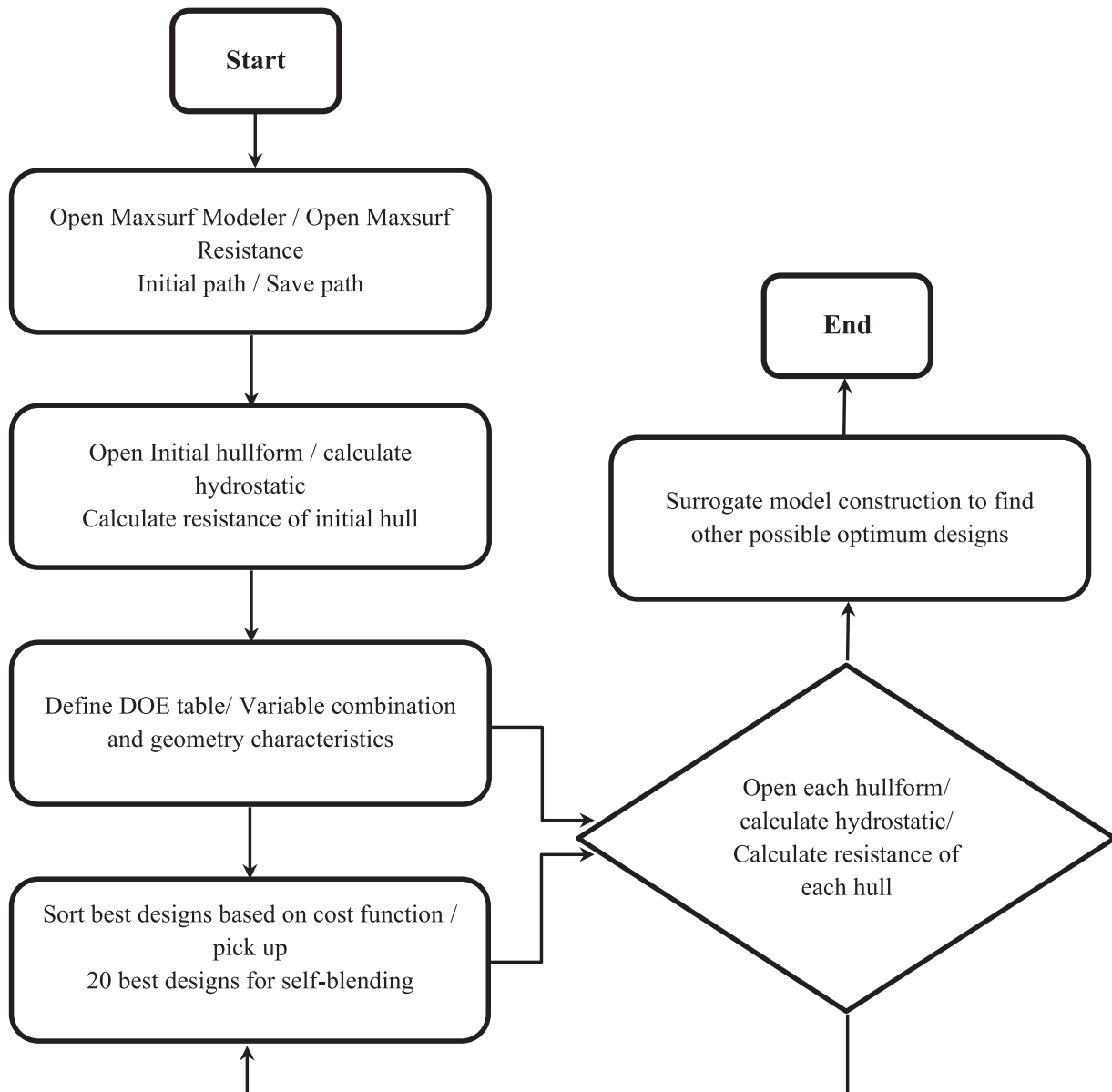


**Figure 8.** Flowchart of the application of the surrogated-based optimisation process. (This figure is available in colour online.)



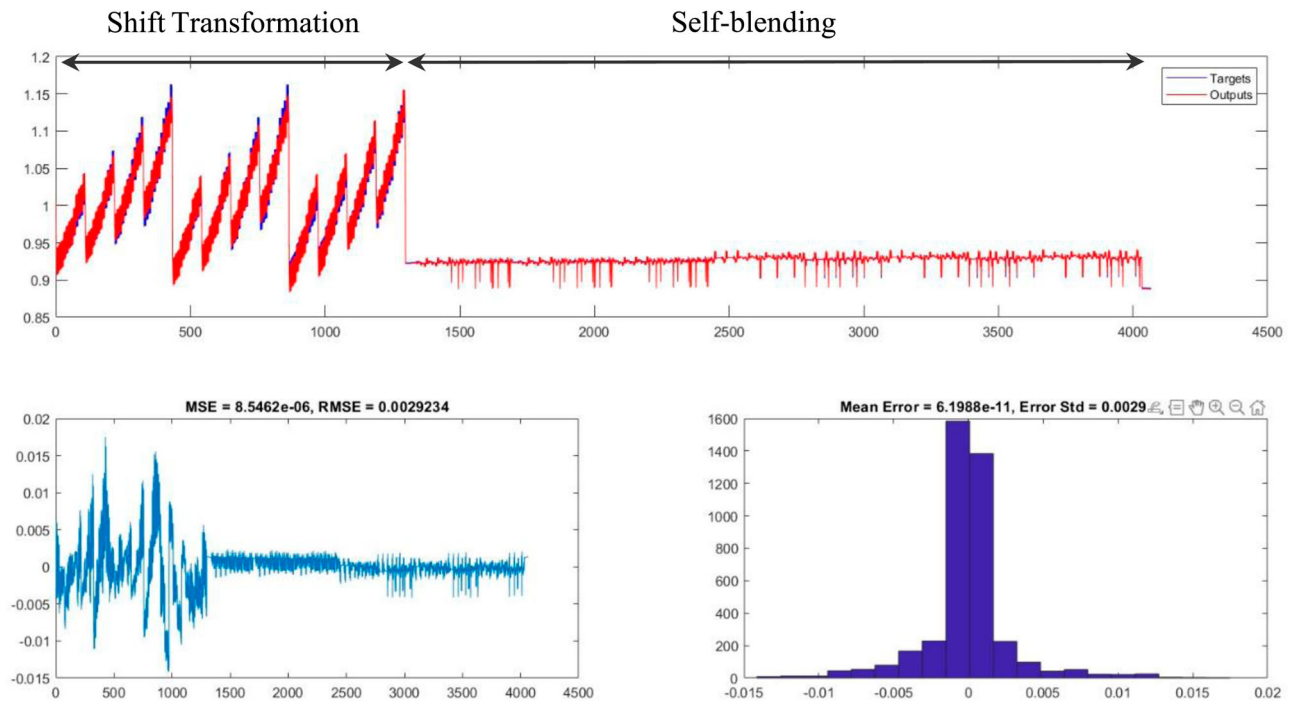


Figure 9. LSM regression on generated designs and model evaluation. (This figure is available in colour online.)

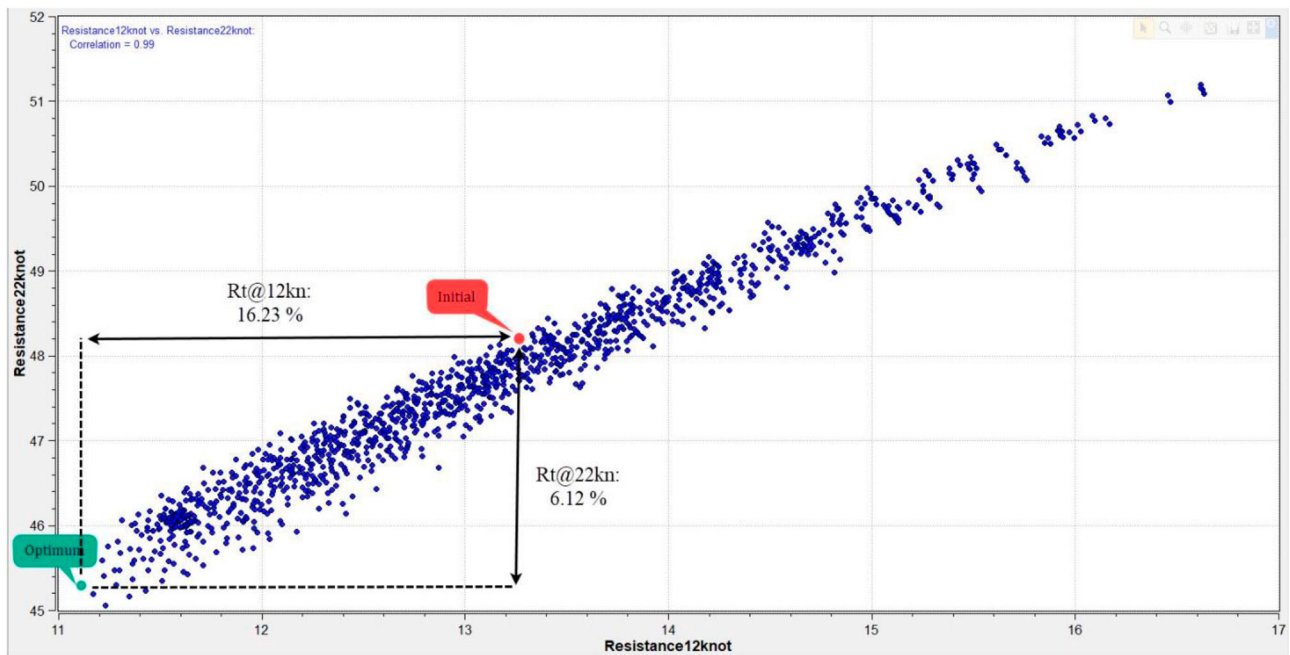


Figure 10. Distribution of generated designs in the design space. (This figure is available in colour online.)

Square method is used to build a regression model and find middle designs. Figure 8 displays the flow chart of this design study. In the first stage, DoE tool distribution generated hulls through Lackenby transformation. These hulls are parent hulls for the blending method that combines two by two. After that, by using the blending method, new hulls are constructed to cover all the design spaces. The proposed combination enhances the construction of the surrogate model, which is defined in stage three of the design study procedure. The obtained metamodel helps to assess the best design based on minimum resistance at multi-design speeds. All the design processes are coded by

MATLAB programming tool. The Matlab code comprises seven sections sequentially from The Component Object Model (COM) interaction between Maxsurf and Matlab to the surrogate model LSM method. The Maxsurf modeller geometry reconstruction and Maxsurf resistance computations are supervised by the Matlab code (Papanikolaou et al. 2010b; Nikolopoulos and Boulogouris 2019; Maxsurf Guide 2020). The connection section, Hydrostatic data extraction, initial design evaluation, DOE table construction, resistance computation, self-blending implementation and surrogate model construction are sequential sections of the code.

**Table 3.** Principal dimensions of the 75-ton new hull catamaran.

Ship particulars	Symbol	Initial design	Optimised design	Improvement
Waterline length (m)	$L_{wl}$	29.844	31	
Total beam (m)	$B$	2.174	2.078	
Draft (m)	$T$	1.2	1.2	
Block coefficient	$C_b$	0.486	0.514	
Midship coefficient	$C_m$	0.776	0.764	
Demi-Hull distance (m)	$DT$	3.4	3.356	
Longitudinal Centre of Buoyancy (m)	LCB (% of L)	0.5185	0.472	
Total breadth (m)	(DT 2)+B	9	8.77	
Resistance@12 knots	$R_{T12}$	13.2633	11.11	16.23%
Resistance@22 knots	$R_{T22}$	48.1784	45.23	6.12%
Cost function	-	1	88.71	11.29%
Displacement (ton)	$\nabla$	75.15	74.5	0.865%

Figure 9 shows 4100 designs of catamarans during the optimisation and regression plot with MSE and RMSE parameters for its evaluation. Figure 10 shows the distributed sample points considering less than one per cent displacement variation. 1296 designs were generated through shift transformation and the best 20 designs were picked up to start the self-blending method. The resistance value at speed 12 knot for the initial design was 13.263 KN which improves by 16.23% and changed to 11.11 KN. Also, the resistance of the initial design at a speed of 22 knots was 48.178 KN, which reduces to 45.233 KN by a 6.12% improvement. Consequently, the cost function of the final optimum design is achieved at 88.71. According to that, the optimisation results indicate an 11.29% hull form optimisation.

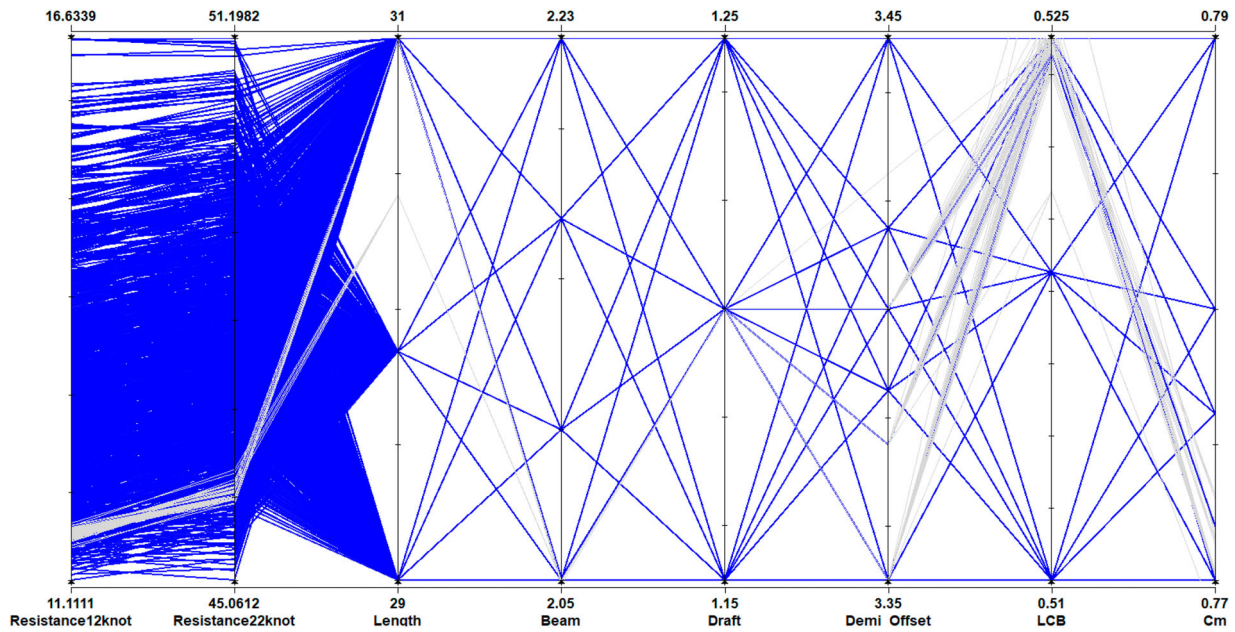


**Figure 11.** Parallel data plot of generated designs for variables and objectives. (This figure is available in colour online.)

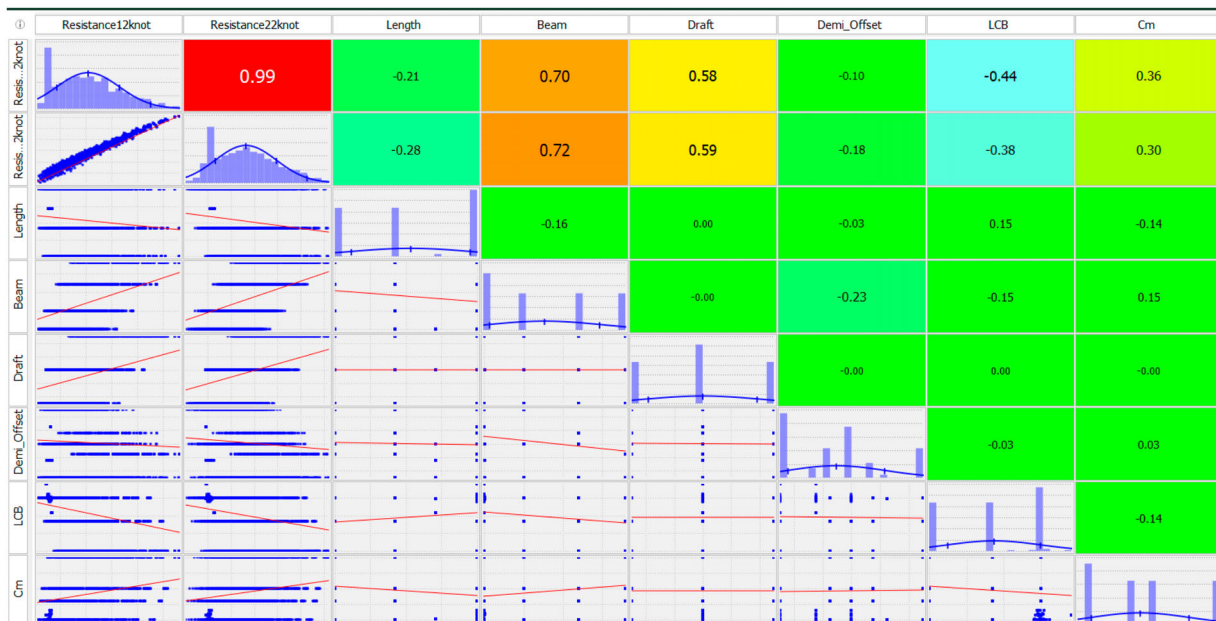


**Figure 12.** Correlation study between design variables and response. (This figure is available in colour online.)

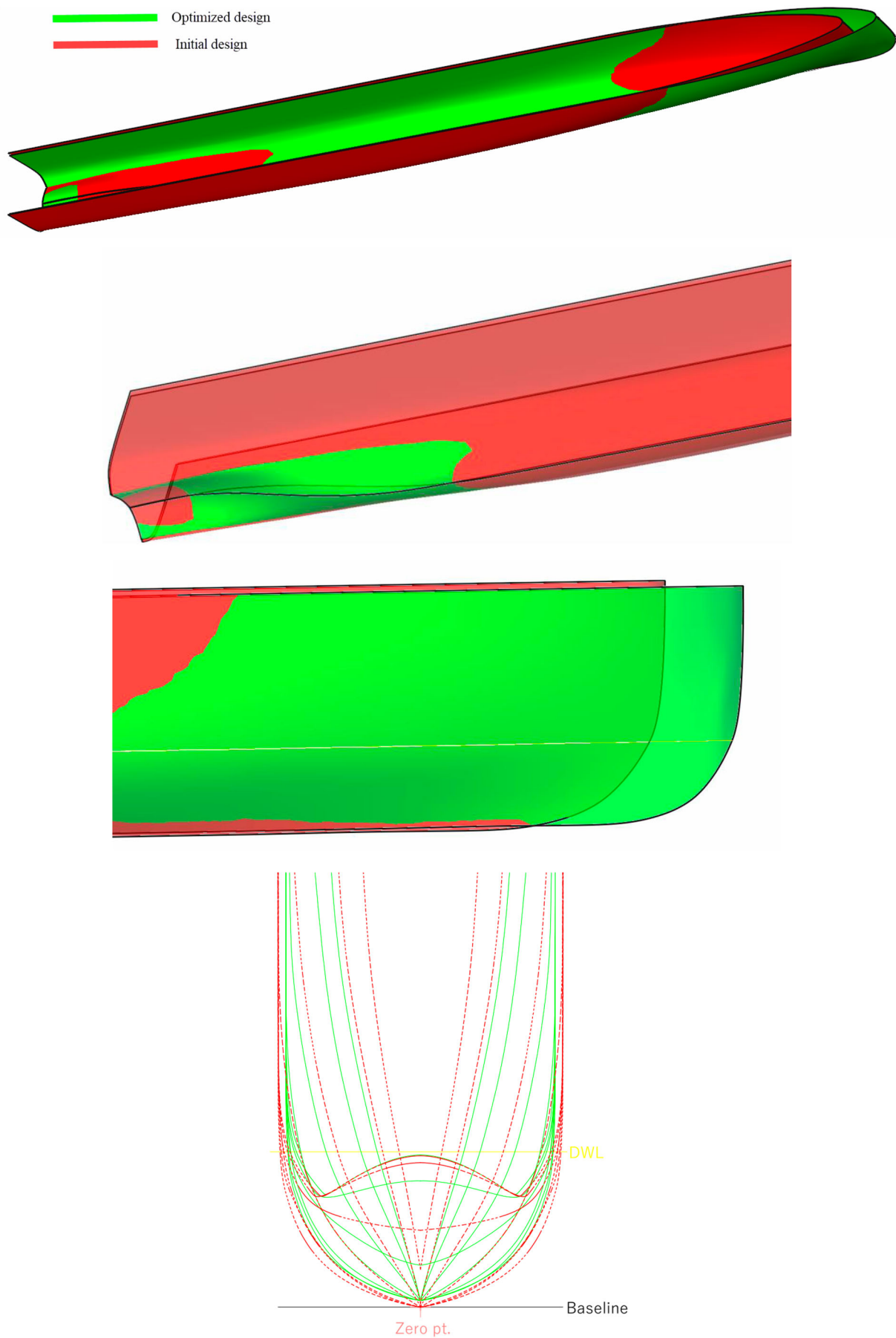


Figure 13. Body plan and 3D view comparison of the initial and optimised hulls. (This figure is available in colour online.)

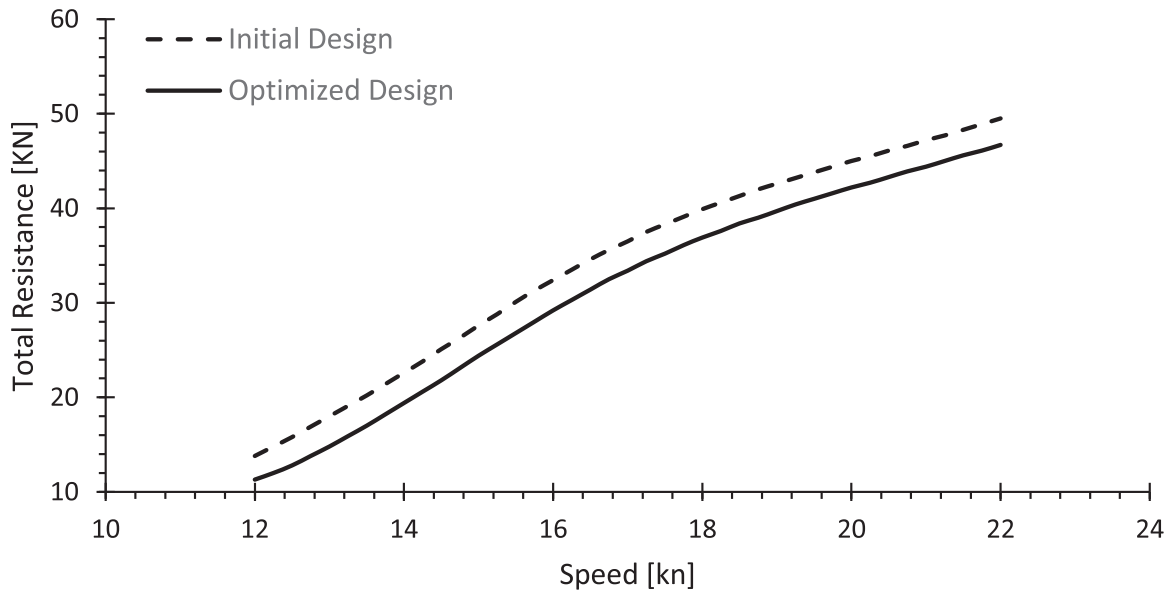


Figure 14. Comparison of total resistance at different speeds between initial and optimised design. (This figure is available in colour online.)

#### 4. Results and discussion

After the deletion of the infeasible designs and design space exploration, the final optimum design has been achieved. A comparison of the initial and optimised values of ship parameters and objective functions is depicted in Table 3. Besides, a parallel data plot presents in Figure 11 to show variable values and corresponding objective values.

The correlation plot represents a better understanding of parameter relation and the effectiveness of variables. Figure 12 displays the correlation plot based on Pearson's correlation coefficient. A high value of 1 (red) indicates a perfect direct linear relationship. A low value of  $-1$  (blue) indicates a perfect inverse linear relationship. Values between high and low values indicate the degree of correlation. A value of 0 (green) indicates no correlation. The most crucial parameter for resistance reduction is Beam at which the correlation value is 0.7 for low-speed resistance and 0.72 for high-speed resistance. It is indicated that further draft reduction yields more resistance reduction. The correlation value for LCB is

negative for both objectives. It could be understood that backward longitudinal shifting of the centre of buoyancy position causes a constructive effect.

Figure 13 displays the body plan and 3D view of the initial and optimised hull. It can be observed in Figure 13 that the length increases in the bow region. The obtained optimisation results illustrate that a lower distance of the bottom curve line in the aft region reduces the resistance. The position of the profile view of the bow region is increased, which changes the pattern of the bow waves.

Figure 14 displays the resistance plot against ship speed for the initial and optimised hull forms. In addition, the wave-making and viscous resistance coefficient are depicted in Figure 15. These plots behave in the same manner for both designs with a similar margin. As shown in Figure 16(a) for the wave pattern around the ship at 12 knots and Figure 16(b) for 22 knots, the computed wave elevation around hulls also reflects the resistance reduction. The optimised hull form generates lower wave amplitudes. Most modifications are performed at the bow shape and bottom of the stern region,

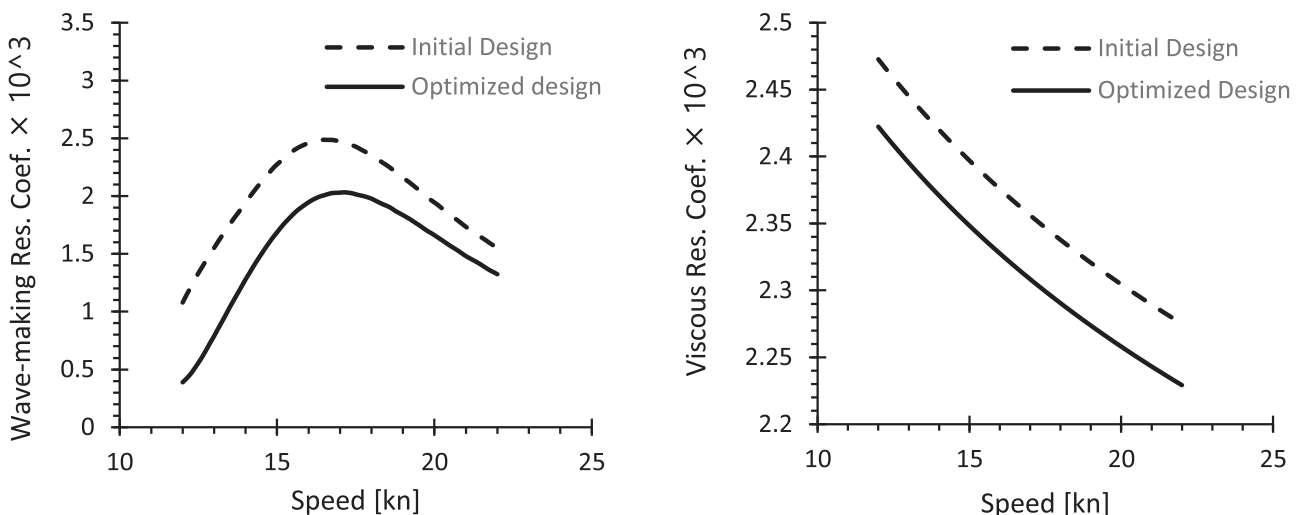
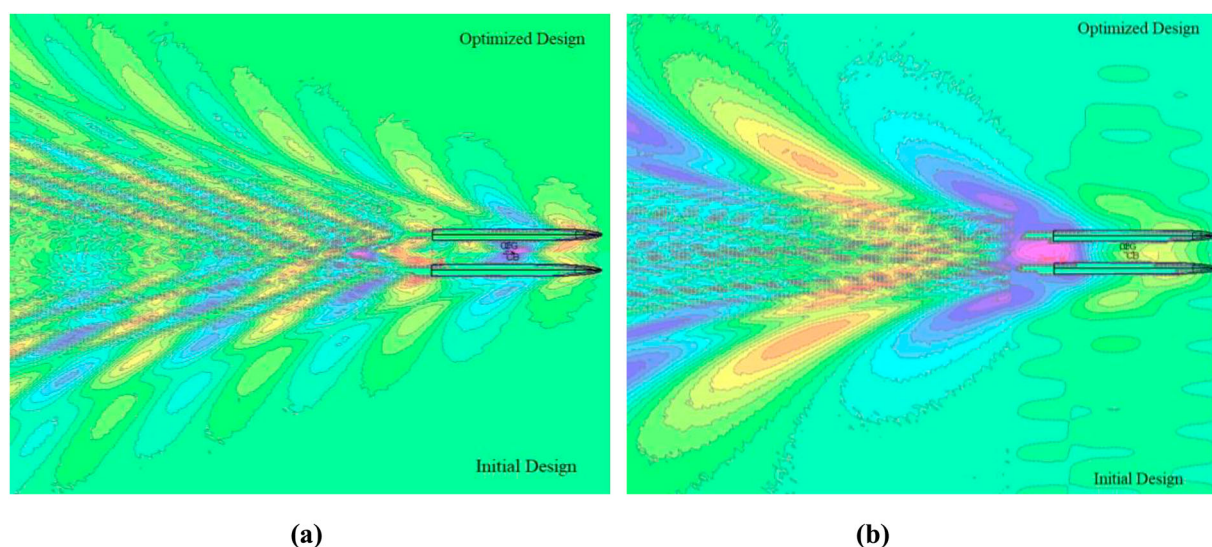


Figure 15. Comparison of wave-making and viscous resistance coefficient at different speeds between initial and optimised designs. (This figure is available in colour online.)



**Figure 16.** Comparison of wave pattern at speeds (a) 12 knots and (b) 22 knots between the initial and optimised designs. (This figure is available in colour online.)

which yields a reduction of the wave amplitudes in the middle and aft portions of the hull, as shown in Figure 16.

## 5. Conclusions

In this paper, a hull form optimisation study is conducted focussing on optimising the ship's resistance. A shift transformation and self-blending method are sequentially applied to alter the hull form. The validity and reliability of the proposed approach are evaluated by using a 31-m catamaran boat as a case study. Furthermore, the advantages and applicability of the proposed method are investigated.

Using the Least Square regression, a larger range of feasible design solutions have been explored in an initial Design of Experiments (DoE). A global geometry optimisation framework is developed herein removing the need to parametrise the geometry. In the first stage, the Lackenby variation method alters the hull forms and multi-level sampling distribution produces initial designs in the design space. After that, the blending method combines the obtained ships to cover the entire design space. Shape modification and change in ship hull geometry are achieved within the constraints of the max total beam of the catamaran and less than 1% change in the displacement. The design variables used in the present study are the length of the waterline, breadth, draft, midship coefficient, longitudinal centre of buoyancy and demi-hull distance. A novel self-blending method is developed based on the control points' displacement. Different combinations of hull surface control points such as axis direction and ship portion are carried out. Control points can be combined in every direction solely ( $X$ ,  $Y$  and  $Z$ ) or combined two by two, such as  $XY$ ,  $XZ$  and  $YZ$ . This scenario was applied at the bow and aft regions of the geometry to investigate the effect of ship part modification on the hull form optimisation.

After the initial design of space exploration, 4100 designs were produced and a surrogate model was constructed on these data. Finally, the optimised design and corresponding design variables are extracted based on the resistance cost function. Resistance at a speed of 12 knots improves by 16.23% and resistance of the initial design at a speed of 22 knots reduces by 6.12%. Accordingly, the cost function of the optimisation problem reduces by 11.26%. Based on the correlation sensitivity study, significant parameters

for the resistance are beam, draft and LCB. It is indicated that an increase in the length leads to a reduction of the resistance. On the contrary, the beam and LCB should be reduced to improve the ship's resistance. The midship section coefficient  $C_m$  is also an important parameter. Lower values of the midship coefficient cause resistance reduction. The obtained optimisation results illustrate a longitudinal shift of the bow region. In addition, the start point of the stern curvature shifts afterwards. A fully automated method without user intervention is the advantage of the present approach. Significant time and effort will be saved to get rid of the parametrisation process and its difficulties. Besides, the two methods' combination and fore, aft and middle parts of ship alterations generate a variety of hull forms, which cover almost the possibility of hull variation. As a result, one may suggest that the present approach of the design study and optimisation leads to a successful approach that can be used in the preliminary stage of the ship design. In addition, the current methodology can be extended to include additional objective functions such as seakeeping and manoeuvring. In addition, a machine learning approach can be developed for different values of blending ratio on each ship section to find a regression model for ship hull optimisation.

## Acknowledgements

The Maritime Safety Research Centre (MSRC) at the University of Strathclyde is an industry–university partnership involving Strathclyde's Department of Naval Architecture, Ocean & Marine Engineering and sponsors of Royal Caribbean Group and DNV. The opinions expressed herein are those of the authors and do not reflect the views of the EU, DNV or RCG.

## Disclosure statement

No potential conflict of interest was reported by the author(s).

## Funding

The TrAM project has received funding from the European Union's Horizon 2020 research and innovation programme under Grant agreement No. 769303.

## ORCID

Amin Nazemian  <http://orcid.org/0000-0001-6861-4488>

## References

- Boulougouris E, Papanikolaou A, Dahle M, Tolo E, Xing Y, Jürgenhake Ch, Seidenberg T, Sachs C, Brown C, Jensen F. 2021. Implementation of zero emission fast shortsea shipping. SNAME Maritime Conference (SMC). Rhode Island, US. <http://dx.doi.org/10.5957/SMC-2021-030>.
- Cong L, Hsiung CC. 1990. A simple method of computing wave resistance, wave profile, and sinkage and trim of transom stern ships. Madrid: ITTC committee.
- Couser P. 1996. An investigation into the performance of high-speed catamarans in calm water and waves [PhD thesis]. Department of Ship Science, University of Southampton.
- Couser P, Wellicome JF, Molland AF. 1998. An improved method for the theoretical prediction of the wave resistance of transom-stern hulls using a slender body approach. *Int Shipbuilding Progr.* 45(444):331–349.
- Deng R, Wang S, Hu Y, Wang Y, Wu T. 2021. The effect of hull form parameters on the hydrodynamic performance of a bulk carrier. *J Marine Sci Eng.* 9(4):373.
- Duman S, Boulougouris E, Aung MZ, Xu X, Nazemian A. 2023. Numerical evaluation of the wave-making resistance of a zero-emission fast passenger ferry operating in shallow water by using the double-body approach. *J Marine Sci Eng.* 11(1):187.
- Eggers K. 1955. Resistance components of two-body ships. *Jahrbuch der Schiffbautechnischen Gesellschaft*; p. 49.
- Feng B, Liu Z, Zhan C, Chang H, Cheng X. 2009. Ship hull automatic optimization techniques research based on CFD. 2009 IEEE 10th International Conference on Computer-Aided Industrial Design & Conceptual Design. p. 663–667.
- Feng Y, Chen Z, Dai Y, Wang F, Cai J, Shen Z. 2018. Multidisciplinary optimization of an offshore aquaculture vessel hull form based on the support vector regression surrogate model. *Ocean Eng.* 166:145–158.
- Ghadimi P, Nazemian A, Ghadimi A. 2019a. Numerical scrutiny of the influence of side hulls arrangement on the motion of a Trimaran vessel in regular waves through CFD analysis. *J Braz Soc Mech Sci Eng.* 41(1):1.
- Ghadimi P, Nazemian A, Sheikholeslami M. 2019b. Numerical simulation of the slamming phenomenon of a wave-piercing trimaran in the presence of irregular waves under various seagoing modes. *Proc Inst Mech Eng Part M J Eng Marit Environ.* 233(4):1198–1211.
- Grigoropoulos GJ, Bakirtzoglou C, Papadakis G, Ntouras D. 2021. Mixed-Fidelity design optimization of hull form using CFD and potential flow solvers. *J Mar Sci Eng.* 9(11):1234.
- Hong ZC, Zong Z, Li HT, Hefazi H, Sahoo PK. 2017. Self-blending method for hull form modification and optimization. *Ocean Eng.* 146:59–69.
- Insel M. 1990. An investigation into the resistance components of high speed displacement catamarans [PhD thesis]. University of Southampton.
- Insel M, Molland AF. 1992. An investigation into the resistance components of high-speed displacement catamarans. Vol. 134. London: Transactions, Royal Institution of Naval Architects; p. 1–20.
- Jeong S, Kim H. 2013. Development of an efficient hull form design exploration framework. *Math Probl Eng.* 2013:27–33. Article ID 838354.
- Kim HJ, Chun HH, Choi HJ. 2007. Development of CFD based stern form optimization method. *J Soc Naval Architects Korea.* 44(6):564–571.
- Lackenby H. 1950. On the systematic geometrical variation of ship forms. *Trans INA.* 92:289–316.
- Li D, Guan Y, Wang Q, Chen Z. 2012. Support vector regression based multidisciplinary design optimization for ship design. *Proceedings naval Conference on Ocean, Offshore and Arctic Engineering, Rio de Janeiro, Brazil.*
- Li D, Wilson PA, Zhao X. 2016. Establishment of effective metamodels for sea-keeping performance in multidisciplinary ship design optimization. *J Mar Sci Technol.* 24(2):233–243.
- Maxsurf Guide. 2020. Maxsurf modeler and automation, User Guide, Version 2020.
- Mitchell JH. 1898. The wave resistance of a ship. *Philos Mag Lond Ser.* 45(5):106–123.
- Mittendorf M, Papanikolaou AD. 2021. Hydrodynamic hull form optimization of fast catamarans using surrogate models. *Ship Technol Res.* 68(1):14–26.
- Nazemian A, Ghadimi P. 2020a. Shape optimisation of trimaran ship hull using CFD-based simulation and adjoint solver. *Ships Offshore Struct.* 17(2):359–373.
- Nazemian A, Ghadimi P. 2020b. Multi-objective optimization of trimaran side-hull arrangement via surrogate-based approach for reducing resistance and improving the seakeeping performance. *Proc Inst Mech Eng Part M J Eng Marit Environ.* 235(4):944–956.
- Nazemian A, Ghadimi P. 2021a. Automated CFD-based optimization of inverted bow shape of a trimaran ship: An applicable and efficient optimization platform. *Sci Iranica.* 28(5):2751–2768.
- Nazemian A, Ghadimi P. 2021b. Global optimization of trimaran hull form to get minimum resistance by slender body method. *J Brazil Soc Mech Sci Eng.* 43(2):67.
- Nazemian A, Ghadimi P. 2021c. CFD-based optimization of a displacement trimaran hull for improving its calm water and wavy condition resistance. *Appl Ocean Res.* 113:102729.
- Nikolopoulos L, Boulougouris E. 2019. Application of holistic ship optimization in bulk carrier design and operation. *Comput Methods Appl Sci.* 48:229–252.
- Papanikolaou A. 2010. Holistic ship design optimization. *Computer-Aided Design.* 42:1028–1044.
- Papanikolaou A, Xing-Kaeding Y, Strobel J, Kanellopoulou A, Zaraphonitis G, Tolo E. 2020. Numerical and experimental optimization study on a fast, zero emission catamaran. *J Mar Sci Eng.* 8(9).
- Papanikolaou A, Zaraphonitis G, Boulougouris E, Langbecker U, Matho S, Sames P. 2010a. Multi-objective optimization of oil tanker design. *J Mar Sci Technol.* 15:359–373.
- Papanikolaou A, Zaraphonitis G, Skoupas S, Boulougouris E. 2010b. An integrated methodology for the design of Ro-Ro passenger ships. *Ship Technol Res.* 57(1):26–39.
- Peri D, Campana EF. 2005. High-fidelity models and multi-objective global optimization algorithms in simulation-based design. *J Ship Res.* 49(3):159–175.
- Peri D, Rossetti M, Campana EF. 2001. Design optimization of ship hulls via CFD techniques. *J Ship Res.* 41:140–149.
- Priftis A, Boulougouris E, Turan O, Atzamos G. 2020. Multi-objective robust early stage ship design optimisation under uncertainty utilising surrogate models. *Ocean Eng* 197:106850.
- Priftis A, Papanikolaou A, Plessas T. 2016. Parametric Design and Multi-objective Optimization of Containerships. *J Ship Prod Des.* 32:1–14.
- Roh MI, Lee KY. 2017. Computational ship design. Singapore: Springer Publication.
- Shi G, Priftis A, Xing Y, et al. 2021. Numerical investigation of the resistance of a zero-emission full-scale fast catamaran in shallow water. *J Mar Sci Eng.* 9(6):563.
- Villa D, Furcas F, Pralits JO, Vernengo G, Gaggero S. 2021. An effective mesh deformation approach for hull shape design by optimization. *J Mar Sci Eng.* 9(10).
- Wang H, Boulougouris E, Theotokatos G, Zhou P, Priftis A, Shi G. 2021. Life cycle analysis and cost assessment of a battery powered ferry. *Ocean Eng.* 241:110029.
- Wigley WCS. 1933. A comparison of experimental and calculated wave-profiles and wave resistances for a form having parabolic waterlines. *R Philos Soc Lond.* 144–159.
- Xing-Kaeding Y, Papanikolaou A. 2021. Optimization of the propulsive efficiency of a fast catamaran. *J Mar Sci Eng.* 9(5):492.
- Yildiz B, Sener B, Duman S, Datla R. 2020. A numerical and experimental study on the outrigger positioning of a trimaran hull in terms of resistance. *Ocean Eng.* 198:106938.
- Zakerdoost H, Ghassemi H, Ghiasi M. 2013. Ship hull form optimization by evolutionary algorithm in order to diminish the drag. *J Mar Sci Appl.* 12(2):170–179.
- Zhang BJ, Zhang SL. 2018. Research on ship design and optimization based on simulation-based design (SBD) technique. Singapore: Springer.
- Zhang G, Wang G, Li X, Ren Y. 2013. Global optimization of reliability design for large ball mill gear transmission based on the Kriging model and genetic algorithm. *Mech Mach Theory.* 69:321–336.
- Zhang S, Zhang B, Tezdogan T, Xu L, Lai Y. 2018. Computational fluid dynamics-based hull form optimization using approximation method. *Eng Appl Comput Fluid Mech.* 12(1):74–88.
- Zong Z, Hong Z, Wang Y, Hefazi H. 2018. Hull form optimization of trimaran using self-blending method. *Appl Ocean Res.* 80:240–247.